Geophysical Research Letters

RESEARCH LETTER
10.1029/2018GL079037

Key Points:
- Additional observations reduced temperature biases at upper troposphere
- Observational signals with smaller uncertainties propagated downstream over the Southern Ocean
- Additional radiosonde observations improved forecast skill of a extratropical cyclone track in the Southern Hemisphere

Supporting Information:
- Supporting Information S1

Correspondence to:
K. Sato,
satokazu@mail.kitami-it.ac.jp

Citation:
Sato, K., Inoue, J., Alexander, S. P., McFarquhar, G., & Yamazaki, A. (2018). Improved reanalysis and prediction of atmospheric fields over the Southern Ocean using campaign-based radiosonde observations. *Geophysical Research Letters*, *45*, 11,406–11,413. https://doi.org/10.1029/2018GL079037

Received 1 JUN 2018
Accepted 27 JUL 2018
Accepted article online 6 AUG 2018
Published online 18 OCT 2018

Improved Reanalysis and Prediction of Atmospheric Fields Over the Southern Ocean Using Campaign-Based Radiosonde Observations

Kazutoshi Sato[1,2], Jun Inoue[3,4,5], Simon P. Alexander[2,6], Greg McFarquhar[7], and Akira Yamazaki[5]

[1]Kitami Institute of Technology, Kitami, Japan, [2]Antarctic Climate and Ecosystems Cooperative Research Centre, Hobart, Tasmania, Australia, [3]National Institute of Polar Research, Tachikawa, Japan, [4]School of Multidisciplinary Sciences, SOKENDAI (Graduate University for Advanced Studies), Hayama, Japan, [5]Application Laboratory, Japan Agency for Marine-Earth Science and Technology, Yokohama, Japan, [6]Australian Antarctic Division, Kingston, Tasmania, Australia, [7]Cooperative Institute for Mesoscale Meteorological Studies and the School of Meteorology, University of Oklahoma, Norman, OK, USA

Abstract This study investigated the impact of radiosonde observations from the Southern Ocean obtained by the Australian R/V *Aurora Australis* on the ALERA2 experimental ensemble reanalysis data set and ensemble forecast experiment. An observing system experiment (OSE) that included additional ship-launched radiosonde data captured the atmospheric structure over the Southern Ocean. ALERA2 without additional radiosondes had positive temperature biases exceeding 7 °C in the upper troposphere when low-pressure cyclonic systems passed over the ship. The spread in the upper level was reduced by 15% in the OSE, which propagated downstream from the ship's position because of the sparse observing network over southern high latitudes. Comparison of two 63-member ensemble forecast experiments initialized by ALERA2 and the OSE revealed that prediction of midlatitude cyclone tracks was improved by the realistic representation of upper-level troughs in the OSE forecast. This confirms that additional radiosondes over the Southern Ocean reduce uncertainty and error in midlatitude cyclone forecasts.

Plain Language Summary Accurate weather forecasts over the Southern Ocean are required for reducing severe damage for ship operations over the high latitudes and social activities over the midlatitudes in the Southern Hemisphere. However, the sparseness of the observing network over the Southern Ocean causes failures in predicting the low-pressure systems. This study investigated the impact of additional observations over the Southern Ocean obtained by the Australian R/V *Aurora Australis* on prediction skill of forecasting systems for weather over the Southern Hemisphere. We revealed that the initial conditions in the reanalysis data, which is used for operational weather forecasts, were improved by the additional radiosonde observations at upper levels, contributing to a more accurate reproduction of a low-pressure system over the midlatitudes in Southern Hemisphere. This confirms that additional radiosondes launched from ships over the Southern Ocean reduce errors in midlatitude cyclone forecasts.

1. Introduction

The density of observing stations and number of observations in polar regions is lower than that in midlatitude and low latitude, causing large errors in reanalysis data (Jung et al., 2016; Jung & Leutbecher, 2007; Jung & Matsueda, 2014). Reanalysis data have large biases not only at the surface (Bracegirdle & Marshall, 2012; Jones & Lister, 2015) but also throughout the troposphere (Jakobson et al., 2012; Jones et al., 2016). The analysis products have temperature and wind biases in the lower troposphere over Antarctica and Southern Ocean (Bromwich et al., 2013; Chen et al., 2014). In addition, in summer, the strength of the trough at 500 hPa over the Southern Ocean in the analysis is weaker than that in analysis with observation data, influencing the development and track of Antarctica cyclone (Chen et al., 2014). Large biases are found at the surface (Bracegirdle & Marshall, 2012; Jones & Lister, 2015) and throughout the troposphere (Jakobson et al., 2012; Jones et al., 2016), even in the reanalysis data. The reanalysis data have large biases in temperature and wind over the Antarctica, in particular in the boundary layer and surface (Jones & Lister, 2015; Nygård et al., 2015; Tastula et al., 2013). In addition, these biases would influence reproductions of the global energy and momentum budgets corresponding to the low-pressure system

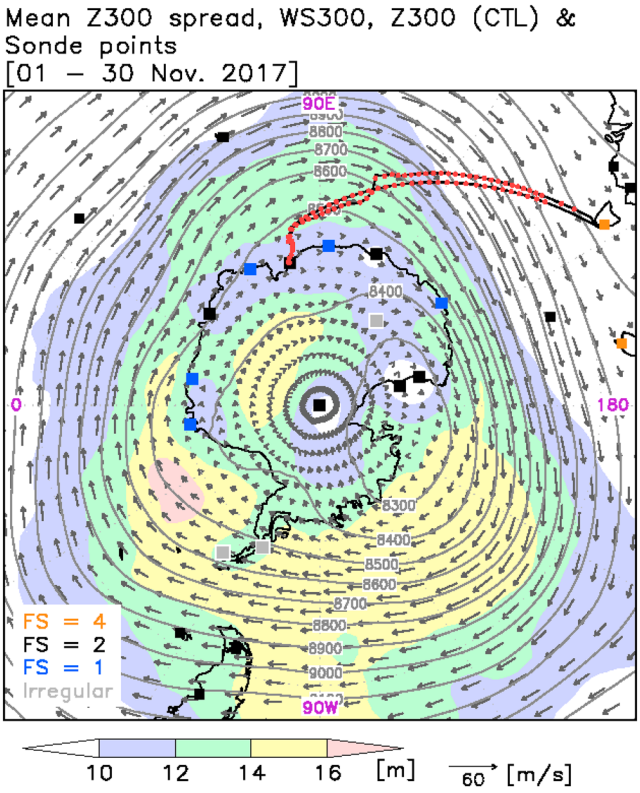

Figure 1. Monthly mean ensemble spread of geopotential height at 300 hPa (Z300) in CTL. Contours and vectors show monthly mean Z300 and wind speed at 300 hPa in CTL. The squares and red dots show radiosonde points of land stations and the R/V AA, respectively, during V1. The colors of squares indicate the frequency of daily radiosonde observations (FS). The black line shows the track of the R/V AA during V1.

(Simmonds & King, 2004). These errors in reanalysis data, which are the same type of analysis data as the initial values used for operational weather forecasts, impact the reproducibility and prediction skill of forecasting systems for weather, oceans, and sea ice (Ono et al., 2016; Yamagami et al., 2017; Yamazaki et al., 2015). In particular, errors over the Southern Ocean are larger than over the Arctic Ocean (Dee et al., 2011; Jung & Matsueda, 2014), even with the incorporation of satellite data. This causes failures in predicting the strong winds associated with low-pressure systems in the Southern Hemisphere, potentially resulting in severe problems for navigation (Wang et al., 2014) and aviation in high latitudes and for a broad range of socio-economic activities in midlatitudes.

The reproducibility of the atmospheric circulation is improved not only by the development of the model itself (Inoue et al., 2011) but also by improvement of the initial states based on additional observations over the polar regions (Inoue et al., 2009, 2013). Over the Arctic region, additional observational data collected by drifting buoys and ship instruments have reduced the error and spread of ensemble members (i.e., uncertainty) in reanalysis products (Inoue et al., 2009, Inoue et al., 2013). Observing system experiments (OSEs) have revealed that additional data acquired by radiosondes and dropsondes over the Arctic Ocean have reduced uncertainty and improved the ensemble mean of upper-level fields. This has contributed to a more accurate reproduction of the surface circulation over both high-latitude and midlatitude areas of the Northern Hemisphere (Inoue et al., 2015; Kristjansson et al., 2011; Sato et al., 2017; Yamazaki et al., 2015). Radiosonde observations have a substantial impact on the reproduction of atmospheric circulation over the downstream area in data-sparse regions, implying that additional observations over the Southern Ocean, where the observation network is sparser than in the Arctic (Jung et al., 2016), should be effective in improving forecast and reanalysis products.

No previous study has reported on the impact of additional Antarctic radiosonde data on weather forecasts over the Southern Hemisphere. Accurate weather forecasts over the Southern Ocean would contribute not only to the safety of ship and aircraft operations to and around the Antarctic but also to the reduction of human and socioeconomic damage over midlatitude areas of the Southern Hemisphere. An Antarctic voyage of the R/V *Aurora Australis* (AA) was conducted in the Southern Ocean during spring 2017 (Figure 1) as part of the Measurement of Aerosols, Radiation and Clouds over the Southern Oceans (MARCUS) project sponsored by the United States Department of Energy. During this voyage, radiosondes were released from the ship to measure vertical profiles of temperature, wind, and humidity. This study considered the impacts of these radiosonde observations over the Southern Ocean on the reproduction and prediction of the atmospheric circulation using an ensemble data assimilation system and OSEs.

2. Data and Method

2.1. MARCUS

The MARCUS project was conducted during austral summer and fall between October 2017 and March 2018 to measure cloud, aerosols, and radiation properties over the Southern Ocean. During this project, the R/V AA made four return crossings of the Southern Ocean. For this study, we used data collected during voyage 1 (V1) during which the R/V AA departed Hobart (43°S, 144°E) on 29 October 2017 and crossed the Southern Ocean to reach Davis (69°S, 78°E) on 13 November (Figure 1). The R/V AA was moored at Davis for cargo operations from 14 to 21 November as well as transiting through sea ice (10–13 and 22–24 November), which enabled evaluation of the reanalyses over sea ice as well as over the Southern Ocean. The R/V AA returned to Hobart on 4 December 2017. During this voyage, radiosondes were launched every 6 hr (00, 06, 12, and 18

UTC) provided sea conditions allowed technicians access to the deck. However, none of these data were sent to the Global Telecommunication System.

Figure 2a shows the time-height cross section of air temperature as measured by the radiosondes during V1. Prior to 10 November and after 24 November, temperatures exceeded 0 °C in the lower troposphere over the Southern Ocean because of northerly winds from the midlatitudes. In contrast, during 10–24 November, the temperature throughout the troposphere over the sea ice around the Antarctic was lower than that measured further north over the Southern Ocean. On 9 and 25 November, temperatures near the tropopause that exceeded −50 °C were found to correspond to cyclone events.

2.2. ALERA2

The atmospheric general circulation model for the Earth Simulator, in combination with the local ensemble transform Kalman filter (AFES-LETKF) ensemble Data Assimilation systems version2 (ALEDAS2), which is an ensemble data assimilation system (Enomoto et al., 2013), was used for evaluating the reanalysis data. ALEDAS2 consists of the AFES (Enomoto et al., 2008; Ohfuchi et al., 2004) and a LETKF (Hunt et al., 2007; Miyoshi & Yamane, 2007). The AFES with horizontal resolution T119 (triangular truncation with truncation wave number 119, ~1° × 1°) and L48 vertical levels (σ-level, up to ~3 hPa) provides 63-member ensemble forecasts. The AFES-LETKF experimental ensemble reanalysis version2 (ALERA2) data sets are produced with ALEDAS2, and they reproduce the geopotential height and temperature structures of synoptic and large-scale circulations in the troposphere and lower stratosphere as well as producing other reanalysis products (Inoue et al., 2013; Sato et al., 2017; Yamazaki et al., 2015). The assimilated observations were adapted from the PREPBUFR Global Observation data sets of the National Centers for Environmental Prediction and archived at the University Corporation for Atmospheric Research. The National Oceanic and Atmospheric Administration daily Optimal Interpolation Sea Surface Temperature (OISST) version 2 data set was used for ocean and sea ice boundary conditions (Reynolds et al., 2007). In this study, we constructed two 63-member ensemble reanalysis data sets. The ALERA2, which includes the observational data in the PREPBUFR global observation data sets, was regarded as the control reanalysis (CTL). The other reanalysis data set comprised an OSE for which radiosonde observational data from the R/V AA were added to the CTL.

The uncertainty of the reanalysis data was estimated using the spread of the 63 members. Figure 1 shows the monthly mean spread of geopotential height at 300 hPa (Z300). Although the spread is large over the Pacific and Atlantic sectors of the Southern Ocean, Weddell Sea, and continental parts of East Antarctica because of the lack of radiosonde observations, the observations acquired by the radiosondes launched routinely from the Antarctic reduce the uncertainty in coastal and central regions. Over the Southern Ocean, radiosonde observations from Tasmania and New Zealand at 6-hr intervals contribute to analysis spread reduction. Thus, radiosonde observations reduce the error and uncertainty of the atmospheric circulation in reanalysis data (Inoue et al., 2015; Sato et al., 2017; Yamazaki et al., 2015). Radiosonde observations onboard the R/V AA were conducted over a region of reasonably large uncertainty in the Southern Ocean; hence, their use was also expected to reduce uncertainty.

3. Results

3.1. Improved Reanalysis Ensemble Mean and Spread at Observation Points

To compare the results of the ensemble reanalysis products with the observations, we selected the grid point nearest the ship position at the time of each radiosonde release. The time-height cross sections of air temperature from the OSE and CTL are shown in Figures 2b and 2c, respectively. Temperatures above 0 °C in the lower troposphere over the Southern Ocean and below −70 °C above the sea ice were reproduced well in both the OSE and the CTL. The OSE captured temperatures exceeding −50 °C at 300 hPa around 9 and 25 November when the R/V AA passed beneath cyclones (Figures 2a and 2b). In contrast, the CTL, which did not assimilate the radiosonde observations from the R/V AA, did not capture the correct temperatures near the tropopause that occurred during the cyclone passages (Figures 2a and 2c). For example, the positive temperature biases exceeded 3 °C near the tropopause on 9 and 25 November (Figure 2d). In particular, on 25 November, the difference was >7 °C. In addition, biases throughout the troposphere between 15 and 21 November (Figures 2d and 2e), that is, when the R/V AA was moored at Davis, are smaller than over the Southern Ocean (Figures 2g and 2h). The transferred routine Davis-based twice-daily radiosonde data in real time to the Global Telecommunication System would reduce biases and spread at the troposphere in

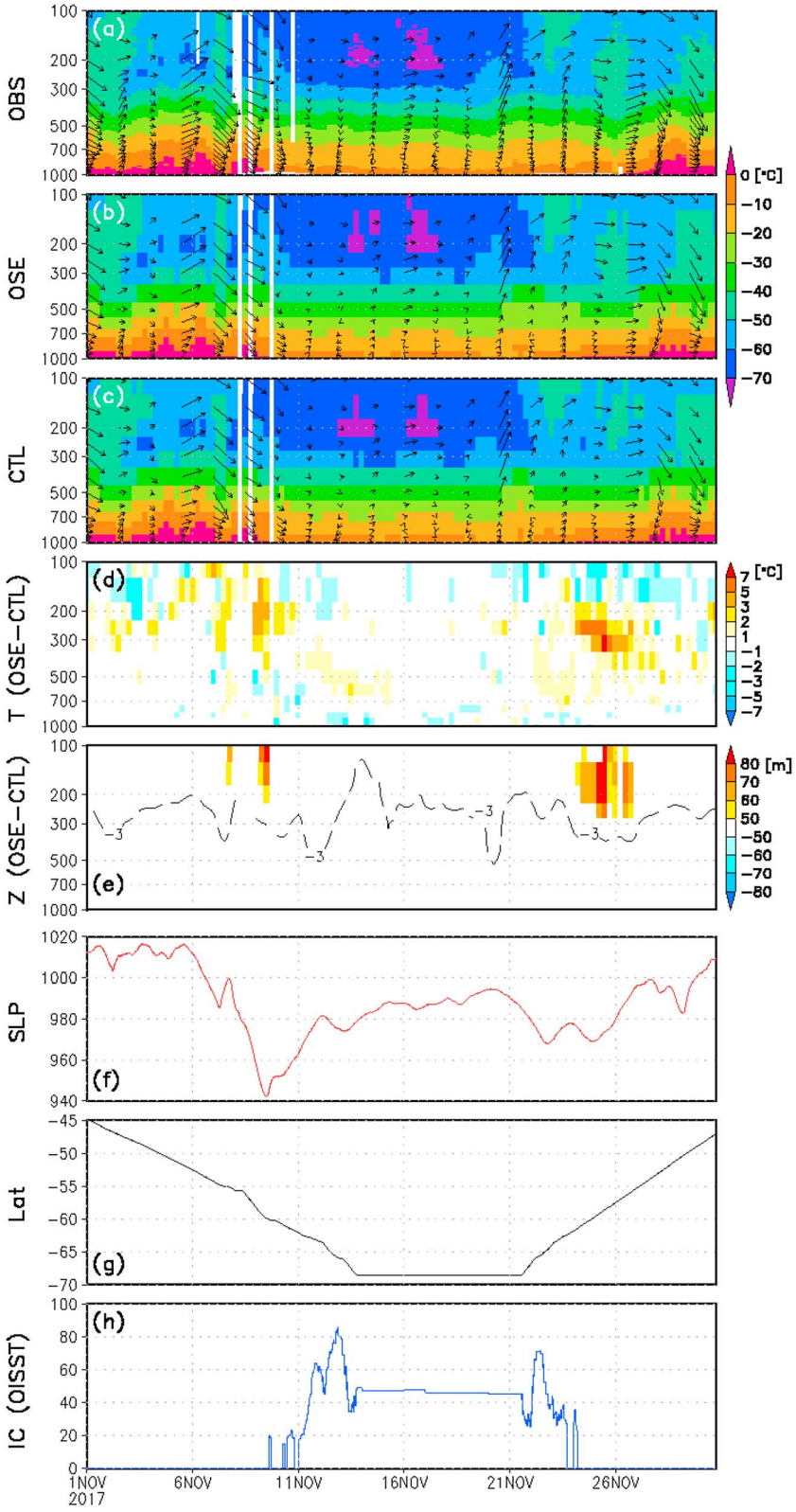

Figure 2. Time-height (pressure: hPa) cross sections of air temperature (shading: °C) and wind speed (vector: m/s) from (a) radiosonde observations, (b) the OSE, and (c) the CTL at the nearest grid point to each radiosonde point. Differences in (d) the ensemble mean temperature (°C) and (e) the ensemble mean (shading: m) and spread (dashed line: m) of geopotential height between the OSE and CTL. Time series of sea level pressure (hPa) at (f) the ship, (g) latitude of the ship, and (h) sea ice cover (%) by OISST at the nearest grid point.

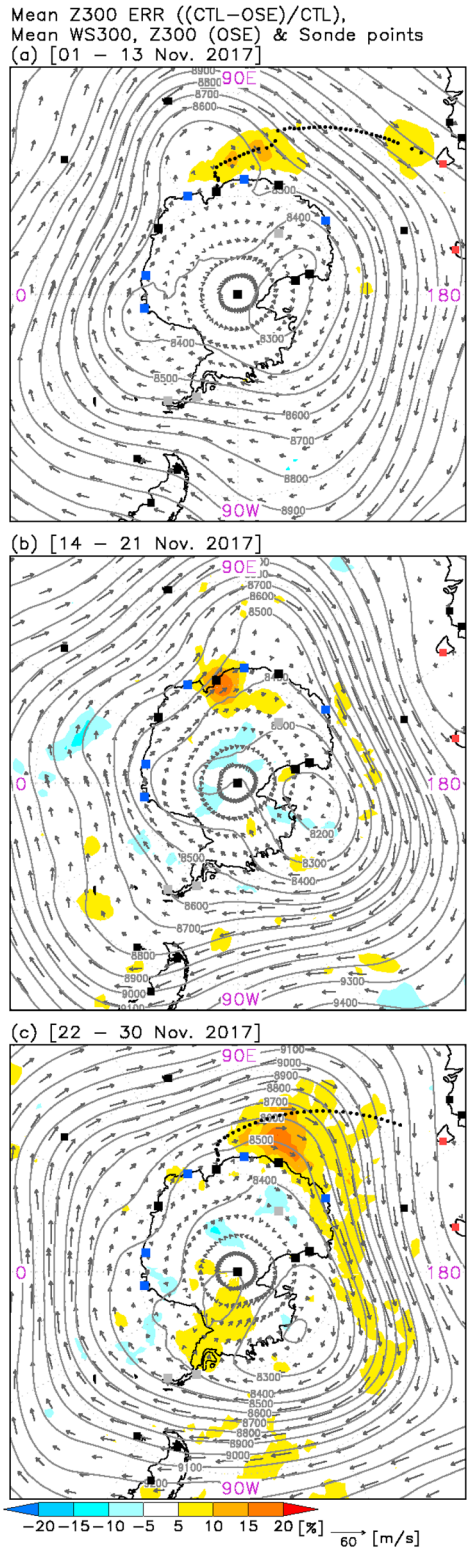

Figure 3. Mean analysis spread reduction rate of Z300 (shading: %), mean analysis Z300 (contour: m), and wind speed (vector: m/s) at 300 hPa in the OSE during (a) period 1 (1–13 November 2017), (b) period 2 (14–21 November 2017), and (c) period 3 (22–30 November 2017). The squares and dots show radiosonde points of land stations and the R/V AA, respectively. The colors of squares indicate the number of daily radiosonde observations.

reanalysis data. Large increments, which are the differences of the ensemble mean temperature (°C) between analysis and first-guess fields, are seen around the tropopause on 9 and 25 November 2017, when low-pressure cyclonic systems passed over the ship (Figure S1), indicating that assimilated additional radiosonde data obtained by the AA are beneficial for improving the temperature in the reanalysis. The time-height cross section of the difference in the ensemble mean and the spread of geopotential height between the OSE and the CTL are shown in Figure 2e. In comparison with the OSE, the CTL has biases (>60 m) and a large ensemble spread (>3 m) of geopotential height above 300 hPa. There is also a difference in geopotential height between the OSE and the CTL when the CTL has positive temperature biases near the tropopause (Figure 2e), implying that the temperature biases are due to the difference of tropopause height between the OSE and the CTL. These biases are most evident when the R/V AA was close to a cyclone (Figure 2f).

In contrast to the upper-level biases, the biases in temperature and geopotential height are less clear in the lower troposphere (Figures 2d and 2e). Biases in the lower troposphere would have been reduced by surface observations at stations located in coastal Antarctica as well as over the Arctic Ocean (Inoue et al., 2009). In addition, biases throughout the troposphere between 15 and 21 November (Figures 2d and 2e), that is, when the R/V AA was moored at Davis, are smaller than over the Southern Ocean (Figures 2g and 2h) because the routine Davis-based twice-daily radiosonde data were transferred in real time to the Global Telecommunication System. However, the difference in spread above 300 hPa still exceeds 3 m, even near the Antarctic stations (Figure 2e), indicating that additional radiosonde observations have a considerable impact on the upper-level atmospheric structure in the reanalysis product. The uncertainty at upper levels in high latitudes tends to be larger than in midlatitude areas because of a lack of observational data, which would be expected to extend downstream because of the sparse observation network over the Southern Ocean.

3.2. Reduced Analysis Ensemble Spread Over Regional and Extended Areas

To investigate the spatial distribution of the improved ensemble spreads attributable to the incorporation of additional radiosonde data, we estimated the analysis error reduction rate (ERR) index (Hattori et al., 2016, 2017; Moteki et al., 2011), which can be defined as

$$\mathrm{ERR} = \frac{\text{spread (CTL)}-\text{spread (OSE)}}{\text{spread (CTL)}} \times 100 \times \frac{Ks}{K},$$

where spread (CTL) and spread (OSE) are the analysis ensemble spread in the CTL and the OSE, respectively. K is the total number of grid points during averaged periods. Ks is the number of grid points which the spread difference exceeded 1 standard deviation. In this study, we focused on the ERR at Z300 as a useful parameter with which to quantify the improvements provided by the incorporation of additional radiosonde observations (Sato et al., 2017).

Figure 3 shows the averaged ERR at Z300 during period 1 (over the Southern Ocean during 1–13 November 2017), period 2 (in fast ice at Davis during 14–21 November 2017), and period 3 (over the Southern

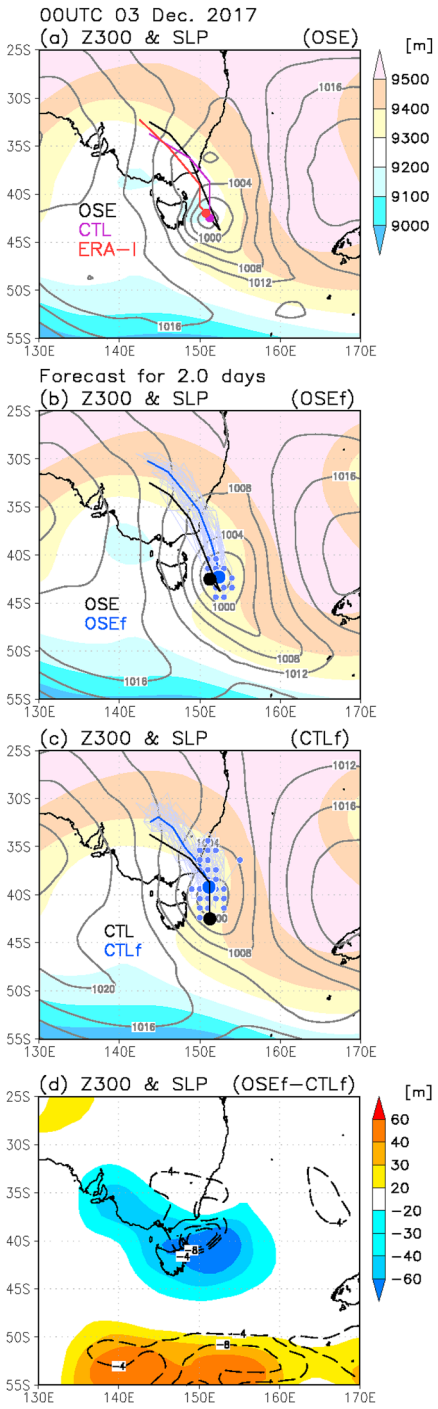

Figure 4. Z300 (shading: m) with SLP (contour: hPa) at 0000 UTC 3 December 2017 in (a) the OSE, (b) OSEf, and (c) CTLf. Differences in mean (shading: m) and spread (contour: m) of Z300 between the OSEf and CTLf are shown in (d). The black, purple, and red lines in (a) show the track of cyclone from 1200 UTC 1 December 2017 through 0000 UTC 3 December 2017 in the OSE, CTL, and ERA-Interim, respectively. The blue thick and thin lines in (b) and (c) show track of cyclone from 1200 UTC 1 December 2017 through 0000 UTC 3 December 2017 in the OSEf and CTLf for the ensemble mean and all ensemble members, respectively. The blue dots in (b) and (c) show location of the cyclone at 1200 UTC 3 December 2017 for the ensemble mean and all ensemble members.

Ocean during 22–30 November 2017). During period 1, the ERR exceeds 5% for observation points near the ship's location over the Southern Ocean (Figure 3a), indicating that additional radiosonde observations reduced the ensemble spread in the reanalysis data. A positive ERR is also seen near the Balleny Islands (67°S, 163°E), where the air sampled over the R/V AA was advected by a westerly wind. During period 2, the R/V AA was anchored near the Davis station (Figure 3b). An ERR exceeding 15% is evident not only near Davis but also extending inland. The area of ERR >5% is limited to high-latitude areas because of the weak westerly wind. In contrast, during period 3, strong westerly winds predominated over the Southern Ocean, leading to widespread positive ERR exceeding 5% from the Southern Ocean to the South Pacific Ocean (Figure 3c). These results suggest that the area of reduced spread depends on the background westerly wind and location in the Southern Ocean.

3.3. Improved Forecast of a Midlatitude Cyclone

The large uncertainty in the reanalysis product used as an initial condition for weather forecasts is expected to affect the prediction skill of atmospheric circulations over the Southern Hemisphere (Inoue et al., 2015; Sato et al., 2017; Yamazaki et al., 2015). To investigate the impact of the incorporation of additional radiosonde data on the prediction of surface systems over midlatitude areas of the Southern Hemisphere, we examined a cyclone that passed near Tasmania during early December 2017. The cyclone developed over southeastern Australia on 1 December and then headed toward the Tasman Sea. The cyclone with a central pressure of 980 hPa was located east of Tasmania on 3 December (Figure 4a), causing heavy precipitation and snowfall over the island. The upper-level trough, influencing the development and track of the cyclone, was located above the western part of the surface cyclone. The strong winds around the trough promoted southward movement of the cyclone. The track of the cyclone in the CTL was similar to the track in the ERA-Interim (Dee et al., 2011), which suggests that ALERA2 is capable of capturing surface circulation systems over the Southern Ocean (Figure 4a). We conducted two ensemble forecasts (hereafter, OSEf and CTLf) using two reanalysis data sets (OSE and CTL) as initial conditions.

The predicted ensemble mean Z300 with SLP for a 2.0-day forecast initialized by the OSE and the CTL reanalysis products at 00 UTC on 1 December is shown in Figures 4b and 4c, respectively. The OSEf captures the center of the cyclone to the east of Tasmania, similar to the result of the ensemble OSE reanalysis (Figure 4b). In contrast, in CTLf, some forecast members placed the center of the cyclone to the northeast of Tasmania (Figure 4c). This discrepancy arises because of the difference in the location of the trough over the Tasman Sea between the OSEf and the CTLf (Figure 4d). In the CTLf, the northward extension of the trough is weaker than in the OSEf, which prevents the cyclone moving as far south. In addition, the location of the cyclone's center in the CTLf (the mean spread of its location is 205 km) is spread more widely compared with the OSEf (the mean spread of its location is 131 km), indicating that the cyclone's location is predicted better in the OSEf than in the CTLf. The large difference in the spread of Z300 between the OSEf and the CTLf suggests that relatively large uncertainty at upper levels leads to the wider spread of cyclone positions in the CTLf. The largest difference of Z300, which provides information regarding the reduced uncertainty attributable to the

incorporation of additional radiosonde observations, was found near the ship observation points at the initial time. The difference moved along the trough over the Southern Ocean with time, and it reached Tasmania at forecast day 2.0 (Figure 4d).

4. Discussion and Conclusions

The present study investigated the impact of additional radiosonde observations over the Southern Ocean on the reproducibility and predictability of atmospheric fields in the Southern Hemisphere. The impact of radiosonde observations launched as part of the MARCUS campaign over the Southern Ocean extended to downstream areas because of the predominant circumpolar westerly wind. Assimilation of MARCUS radiosonde data improved the reproducibility of an upper-level trough and surface circulation, and it modified the track of a cyclone near Tasmania (Figure 4a). The reanalysis data have larger uncertainty and error in the lower troposphere above sea ice over the Antarctic, in comparison with the Arctic, because of the sparser surface observation network in the Antarctic region (Inoue et al., 2009; Jakobson et al., 2012; Jones & Lister, 2015). In addition, our data denial experiments showed that the additional MARCUS radiosonde data improved the ensemble mean and spread at upper levels in reanalysis data, partly because an upper trough is important for the development of the surface circulation (Keable et al., 2002; Lim & Simmonds, 2007; Simmonds & Lim, 2009; Simmonds & Rudeva, 2014).

Antarctic research and resupply voyages are generally conducted during late spring and summer. While some of these vessels have the ability to launch radiosondes, cost and logistical limitations will probably limit Southern Ocean ship-based radiosonde launches to campaigns for the foreseeable future. However, an alternative would be to use the year-round, high-resolution vertical profiles of wind speeds obtained by VHF wind-profiling radars throughout the troposphere and into the stratosphere at various coastal East Antarctic locations (Alexander et al., 2017; Sato et al., 2014). These data can be used to evaluate forecasts (Alexander et al., 2017) and may also enable improvement of reanalysis data. In addition, the skill of weather forecasts over the midlatitudes can be improved by the incorporation of observations not only from the polar region but also from tropical regions. Jung et al. (2014) previously reported that improvements in the representation of atmospheric circulations over high- and low-latitude regions at initial times enhance the accuracy of predictions over the midlatitudes. Therefore, it is likely that the forecast skill of atmospheric circulations over the Southern Hemisphere midlatitudes should also be improved by the incorporation of additional radiosonde observations from tropical regions through teleconnections (Hattori et al., 2017; Irving & Simmonds, 2016). As part of the activities of the Year of Polar Prediction and the Year of Maritime Continents programs, from mid-2017 to mid-2019, an enhanced radiosonde observational network will be established. It will provide the opportunity to investigate the importance of additional tropical and Antarctic radiosonde observations on the reproducibility of observed atmospheric circulation over the Southern Hemisphere midlatitudes.

Acknowledgments
This work was supported by the JSPS Overseas Research Fellowship, JSPS KAKENHI (Grant 18H05053), Australian Antarctic Science Project 4292, U.S. Department of Energy Award (DE-SC0018626), and U.S. National Science Foundation (grants 1628674 and 1762096). We would like to thank anonymous reviewers whose constructive comments improved the quality of this manuscript. Technical, logistical, and ship support for MARCUS were provided by the Australian Antarctic Division. MARCUS data were obtained from the Atmospheric Radiation Measurement (ARM) Program sponsored by the U.S. Department of Energy, Office of Science, Office of Biological and Environmental Research, and Climate and Environmental Sciences Division. We thank all the ARM technicians who collected the radiosonde data onboard R/V *Aurora Australis*. ALEDAS2 and AFES integrations were performed on the Earth Simulator with the support of JAMSTEC. PREPBUFR data, compiled by the National Centers for Environmental Prediction (NCEP) and archived at the University Corporation for Atmospheric Research (UCAR), were used as the observations (available from http://rda.ucar.edu). The data sets provided by ALEDAS2 were used from JAMSTEC web site (http://www.jamstec.go.jp/alera/alera2.html). We thank James Buxton MSc from Edanz Group (www.edanzediting.com./ac) for correcting a draft of this manuscript.

References

Alexander, S. P., Orr, A., Webster, S., & Murphy, D. J. (2017). Observations and fine-scale model simulations of gravity waves over Davis, East Antarctica (69°S, 78°E). *Journal of Geophysical Research: Atmospheres*, *122*, 7355–7370. https://doi.org/10.1002/2017JD026615

Bracegirdle, T. J., & Marshall, G. J. (2012). The reliability of Antarctic tropospheric pressure and temperature in the latest global reanalyses. *Journal of Climate*, *25*(20), 7138–7146. https://doi.org/10.1175/JCLI-D-11-00685.1

Bromwich, D. H., Otieno, F. O., Hines, K. M., Manning, K. W., & Shilo, E. (2013). Comprehensive evaluation of polar weather research and forecasting performance in the Antarctic. *Journal of Geophysical Research: Atmospheres*, *118*, 274–292. https://doi.org/10.1029/2012JD018139

Chen, S.-Y., Wee, T.-K., Kuo, Y.-H., & Bromwich, D. H. (2014). An impact assessment of GPS radio occultation data on prediction of a rapidly developing cyclone over the Southern Ocean. *Monthly Weather Review*, *142*(11), 4187–4206. https://doi.org/10.1175/MWR-D-14-00024.1

Dee, D. P., Uppala, S. M., Simmons, A. J., Berrisford, P., Poli, P., Kobayashi, S., et al. (2011). The ERA-interim reanalysis: Configuration and performance of the data assimilation system. *Quarterly Journal of the Royal Meteorological Society*, *137*(656), 553–597. https://doi.org/10.1002/qj.828

Enomoto, T., Kuwano-Yoshida, A., Komori, N., & Ofuchi, W. (2008). Description of AFES 2: Improvements for high-resolution and coupled simulations. In K. Hamilton, & W. Ohfuchi (Eds.), *High resolution numerical modelling of the atmosphere and ocean* edited by (pp. 77–97). New York: Springer.

Enomoto, T., Miyoshi, T., Moteki, Q., Inoue, J., Hattori, M., Kuwano-Yoshida, S., et al. (2013). Observing-system research and ensemble data assimilation at JAMSTEC. In S. K. Park, & L. Xu (Eds.), *Data assimilation for atmospheric, oceanic and hydrologic applications (Vol. II)* edited by (pp. 509–526). Berlin Heidelberg: Springer.

Hattori, M., Matsumoto, J., Ogino, S., Enomoto, T., & Miyoshi, T. (2016). The impact of additional radiosonde observations on the analysis of disturbances in the South China Sea during VPREX2010. *SOLA*, *12*(0), 75–79. https://doi.org/10.2151/sola.2016-018

Hattori, M., Yamazaki, A., Ogino, A., Wu, P.-M., & Matsumoto, J. (2017). Impact of the radiosonde observations of cold surge over the Philippine Sea on the tropical region and the Southern Hemisphere in December 2012. *SOLA*, *13*(0), 19–24. https://doi.org/10.2151/sola.2017-004

Hunt, B. R., Kostelich, E. J., & Szunyogh, I. (2007). Efficient data assimilation for spatiotemporal chaos: A local ensemble transform Kalman filter. *Physica D*, *230*(1-2), 112–126. https://doi.org/10.1016/j.physd.2006.11.008

Inoue, J., Enomoto, T., & Hori, M. E. (2013). The impact of radiosonde data over the ice-free Arctic Ocean on the atmospheric circulation in the Northern Hemisphere. *Geophysical Research Letters*, *40*, 864–869. https://doi.org/10.1002/grl.50207

Inoue, J., Enomoto, T., Miyoshi, T., & Yamane, S. (2009). Impact of observations from Arctic drifting buoys on the reanalysis of surface fields. *Geophysical Research Letters*, *36*, L08501. https://doi.org/10.1029/2009GL037380

Inoue, J., Hori, M. E., Enomoto, T., & Kikuchi, T. (2011). Intercomparison of surface heat transfer near the Arctic marginal ice zone for multiple reanalyses: A case study of September 2009. *SOLA*, *7*, 57–60. https://doi.org/10.2151/sola.2011-015

Inoue, J., Yamazaki, A., Ono, J., Dethloff, K., Maturilli, M., Neuber, R., et al. (2015). Additional Arctic observations improve weather and sea-ice forecasts for the Northern Sea Route. *Scientific Reports*, *5*(1), 16868. https://doi.org/10.1038/srep16868

Irving, D., & Simmonds, I. (2016). A new method for identifying the Pacific-South American pattern and its influence on regional climate variability. *Journal of Climate*, *29*(17), 6109–6125. https://doi.org/10.1175/JCLI-D-15-0843.1

Jakobson, E., Vihma, T., Palo, T., Jakobson, L., Keernik, H., & Jaagus, J. (2012). Validation of atmospheric reanalyses over the central Arctic Ocean. *Geophysical Research Letters*, *39*, L10802. https://doi.org/10.1029/2012GL051591

Jones, P. D., & Lister, D. H. (2015). Antarctic near-surface air temperatures compared with ERA-Interim values since 1979. *International Journal of Climatology*, *35*(7), 1354–1366. https://doi.org/10.1002/joc.4061

Jones, R. W., Renfrew, I. A., Orr, A., Webber, B. G. M., Holland, D. M., & Lazzara, M. A. (2016). Evaluation of four global reanalysis products using in situ observations in the Amundsen Sea Embayment, Antarctica. *Journal of Geophysical Research: Atmospheres*, *121*, 6240–6257. https://doi.org/10.1002/2015JD024680

Jung, T., Gordon, N. D., Bauer, P., Bromwich, D. H., Chevallier, M., Day, J. J., et al. (2016). Advancing polar prediction capabilities on daily to seasonal time scales. *Bulletin of the American Meteorological Society*, *97*(9), 1631–1647. https://doi.org/10.1175/BAMS-D-14-00246.1

Jung, T., Kasper, M. A., Semmler, T., & Serrar, S. (2014). Arctic influence on subseasonal midlatitude prediction. *Geophysical Research Letters*, *41*, 3676–3680. https://doi.org/10.1002/2014GL059961

Jung, T., & Leutbecher, M. (2007). Performance of the ECMWF forecasting system in the Arctic during winter. *Quarterly Journal of the Royal Meteorological Society*, *133*(626), 1327–1340. https://doi.org/10.1002/qj.99

Jung, T., & Matsueda, M. (2014). Verification of global numerical weather forecasting systems in polar regions using TIGGE data. *Quarterly Journal of the Royal Meteorological Society*, *142*, 574–582.

Keable, M., Simmonds, I., & Keay, K. (2002). Distribution and temporal variability of 500 hPa cyclone characteristics in the Southern Hemisphere. *International Journal of Climatology*, *22*(2), 131–150. https://doi.org/10.1002/joc.728

Kristjansson, J. E., et al. (2011). The Norwegian IPY-THOPEX: Polar lows and Arctic fronts during the 2008 Andøya Campaign. *Bulletin of the American Meteorological Society*, *92*(11), 1443–1466. https://doi.org/10.1175/2011BAMS2901.1

Lim, E.-P., & Simmonds, I. (2007). Southern Hemisphere winter extratro-pical cyclone characteristics and vertical organization observed with the ERA-40 reanalysis data in 1979–2001. *Journal of Climate*, *20*(11), 2675–2690. https://doi.org/10.1175/JCLI4135.1

Miyoshi, T., & Yamane, S. (2007). Local ensemble transform Kalman filtering with an AGCM at a T159/L48 resolution. *Monthly Weather Review*, *135*(11), 3841–3861. https://doi.org/10.1175/2007MWR1873.1

Moteki, Q., Yoneyama, K., Shirooka, R., Kubota, H., Yasunaga, K., Suzuki, J., et al. (2011). The influence of observations propagated by convectively coupled equatorial waves. *Quarterly Journal of the Royal Meteorological Society*, *137*(656), 641–655. https://doi.org/10.1002/qj.779

Nygård, T., Vihma, T., Birnbaum, G., Hartmann, J., King, J., Lachlan-Cope, T., et al. (2015). Validation of eight atmospheric reanalyses in the Antarctic peninsula region. *Quarterly Journal of the Royal Meteorological Society*, *142*(695), 684–692. https://doi.org/10.1002/qj.2691

Ohfuchi, W., Nakamura, H., Yoshioka, M. K., Enomoto, T., Takaya, K., Peng, X., et al. (2004). 10- km mesh meso-scale resolving simulations of the global atmosphere on the Earth Simulator-Preliminary outcomes of AFES (AGCM for the Earth Simulator). *Journal of the Earth Simulator*, *1*, 8–34.

Ono, J., Inoue, J., Yamazaki, A., Dethloff, K., & Yamaguchi, H. (2016). The impact of radiosonde data on forecasting sea-ice distribution along the Northern Sea Route during an extremely developed cyclone. *Journal of Advances in Modeling Earth Systems*, *8*, 292–303. https://doi.org/10.1002/2015MS000552

Reynolds, R. W., Smith, T. M., Liu, C., Chelton, D. B., Casey, K. S., & Schlax, M. G. (2007). Daily high-resolution-blended analyses for sea surface temperature. *Journal of Climate*, *20*(22), 5473–5496. https://doi.org/10.1175/2007JCLI1824.1

Sato, K., Inoue, J., Yamazaki, A., Kim, J.-H., Maturilli, M., Dethloff, K., et al. (2017). Improved forecasts of winter weather extremes over midlatitudes with extra Arctic observations. *Journal of Geophysical Research: Oceans*, *122*, 775–787. https://doi.org/10.1002/2016JC012197

Sato, K., Tsutsumi, M., Sato, T., Nakamura, T., Saito, A., Tomikawa, Y., et al. (2014). Program of the Antarctic Syowa MST/IS Radar (PANSY). *Journal of Atmospheric and Solar - Terrestrial Physics*, *118*, 2–15. https://doi.org/10.1016/j.jastp.2013.08.022

Simmonds, I., & King, J. C. (2004). Global and hemispheric climate variations affecting the Southern Ocean. *Antarctic Science*, *16*(4), 401–413. https://doi.org/10.1017/S0954102004002226

Simmonds, I., & Lim, E. P. (2009). Biases in the calculation of Southern Hemisphere mean baroclinic eddy growth rate. *Geophysical Research Letters*, *36*, L01707. https://doi.org/10.1029/2008GL036320

Simmonds, I., & Rudeva, I. (2014). A comparison of tracking methods for extreme cyclones in the Arctic basin. *Tellus*, *66A*, 25252.

Tastula, E.-M., Vihma, T., Andreas, E. L., & Galperin, B. (2013). Validation of the diurnal cycles in atmospheric reanalyses over Antarctic sea ice. *Journal of Geophysical Research: Atmospheres*, *118*, 4194–4204. https://doi.org/10.1002/jgrd.50336

Wang, Z., Turner, J., Sun, B., Li, B., & Liu, C. (2014). Cyclone-induced rapid creation of extreme Antarctic sea ice conditions. *Scientific Reports*, *4*(1), 5317. https://doi.org/10.1038/srep05317

Yamagami, A., Matsueda, M., & Tanaka, H. L. (2017). Extreme arctic cyclone in August 2016. *Atmospheric Science Letters*, *18*(7), 307–314. https://doi.org/10.1002/asl.757

Yamazaki, A., Inoue, J., Dethloff, K., Maturilli, M., & Konig-Langlo, G. (2015). Impact of radiosonde observations on forecasting summertime Arctic cyclone formation. *Journal of Geophysical Research: Atmospheres*, *120*, 3249–3273. https://doi.org/10.1002/2014JD022925